Chapter

Stabilized Graphene Oxide Assisted Surfactants and Its Capacitance Performance

Nurhafizah Md Disa

Abstract

The use of surfactant in achieving high stabilization and exfoliation graphene oxide (GO) was seen to be the crucial factor in improving the quality and quantity of GO produced via electrochemical exfoliation method. Therefore, this chapter is presenting the physical characterizations that successfully showed the stabilization of GO by various anionic surfactant. The uniqueness in this work was lie on the number of tails surfactant which consists of single-, double- and triple-tails, and the comparison study in terms of electrical conductivity between the commercial and custom-made surfactants. Moreover, the effective stabilized-GO was further explored in super capacitor application. This work opens a new window for green and low-cost GO material as conductive electrodes material.

Keywords: graphene oxide, surfactant, electrical conductivity, supercapacitor

1. Introduction

In 2004, Graphene (GE) has evolved as an interesting two-dimensional gapless semiconductor material [1]. GE is suitable for many technological applications due to the fascinating properties such as high mobility of charge carriers, large surface area calculated up to 2630 m^2g^{-1}, high mechanical strength (young modulus ~ 1 Tpa), excellent thermal conductivity and almost transparent [2–5]. However, the issue of graphene's price due to the world energy crisis intensively affects the national progress of developing countries, because it weighed down all sectors, such as in economy, industry, agriculture, social life and inflation to poverty, hence national progress slow down. The demand of GE has gained attention even though the price is tremendously increased year by year and the price predicted to exceed USD 200 million by 2024 according to Global Market Insight, Inc. The increasing factors are due to the demands from various industries including automotive, aerospace and electronics. Thus, the implementation of its derivative from the graphene's family is highly needed to cater the economy issue. Thus, in recent years, Graphene oxide (GO), and reduced GO (rGO) have gained much attention due to its superb properties. The existence of oxygen content that is bonded on the surfaces and edges part of GO sheets is important for functionalization purpose. So far, various techniques were carried out to produce GO from various carbon sources such as scotch tape, CVD, chemical reduction process as well as carbonization of natural sources. Because of that, the development of methods that allow the mass

production of excellent quality graphene materials has become a top priority today. The GO material is now emerging from the laboratory into the commercial product, soon our nation will be recognized as a key player involved in this frontier technology. However, the prevention of aggregation was of particular importance for GE sheets because most of their unique properties were only associated with individual sheets and keeping them well separated was required. Researchers have found that the maximum improvement of GE properties can totally be seen by compositing GE along with other conducting materials such as carbon nanotubes (CNTs) in a small quantity [6].

To date, GE dispersions in the polymer matrix performed higher electrical properties which beyond the mixing of two conventional nanofillers namely silicates and carbon nanotubes (CNTs) [7, 8]. However, the highly restacking GE-based materials due to the strong van der Waals interactions between the GE sheets, led this kind of materials to have low solubility in the polymer matrix. This paved the way to introduce such interfacial adhesion in order to produce finely dispersed GE-based materials in polymer matrices and believed to improve the nanocomposite conductivity [9–12].

Therefore, the use of non-functionalization of surfactant to assist GE-based materials dispersions in the nanocomposite was currently employed and reported to highly preserve the properties of nanofillers in the nanocomposite as compared to covalent modifications [13, 14]. In addition, the existence of the excess surfactant in the nanocomposite was highly affected the electrical conductivity of the end-product of nanocomposite even though some researchers reported that the surfactant hinder the electron movement of GE in the nanocomposite [15]. Apart from that, the number of tail group of surfactant was also seen to have an important impact to produce better dispersion subsequently, leading to increased electrical conductivity [14]. They prepared the thermally reduced GO (TRGO) using annealing process at temperature of about ~1000°C which further stabilized by ionic sodium dodecyl sulfate (SDS) and non-ionic (Pluronic F 127) surfactants. The nanocomposite was obtained by means of latex technology and showed higher electrical percolation threshold of around 10^{-6} S cm^{-1} (SDS) as compared to Pluronic F127 stabilized in TRGO/natural rubber latex (NRL) polymer nanocomposite (~10^{-9} S cm^{-1}). This results further gives information that the ionic SDS surfactant is an effective surfactant in stabilizing GE-based materials led in good dispersion of nanocomposite produced.

In addition, Mohamed et al. [16, 17] also demonstrated the electrical improvements of the CNTs/NRL polymer nanocomposite by increasing the number of tail group of surfactant from single- (SDS) to double- (AOT4) and triple-chain (TC14). They found that electrical enhancement was increased up to ~× 10^{-3} S cm^{-1} for the CNTs/NRL polymer nanocomposite assisted TC14 as compared to pure NRL (σ = ~10^{-11} S cm^{-1}). Due to surfactant stabilization theory of CNTs-based nanocomposite was similar to the GE-based nanocomposite, the probability similar effect of GE-based materials dispersion filled in the NRL polymer with the assisted various number of tail groups might also led to the significant improvement in the electrical conductivity and capacitance performance.

Until now, the lack of studies regarding to the properties and intermolecular interactions of GE assisted various number of surfactant tail groups in the nanocomposite has made this field loosely explored. Moreover, GE-based materials always show re-stacking properties when forming an agglomeration structures. Due to the inaccessible site for ions diffusion in restacking agglomerate GO, the use of so-called non-functionalization of surfactants were demonstrated to encounter the excess agglomerated sheets in the nanocomposite electrode materials. With the addition of surfactants for stabilizing GO or rGO sheets during fabrication

process in the nanocomposite, researchers have found the effective SDBS as stabilized agent in the nanocomposite which performed the highest stability using *C-V* measurement [18]. Yuan et al. also demonstrated the higher specific capacitance of 690 F g^{-1} in the presence of SDBS-stabilized GE with PANI as electrodes materials in supercapacitor [19]. In addition, Jothi et al. obtained 1312 F g^{-1} of capacitance performance by applying pluoronic P123 in the hybridization between rGO and nanoporous nickel sulfide [20]. They reported three main factors which contribute to the high capacitance performance, including: (i) high porous structure of material, (ii) uniform surface coating and (iii) reduced stacking effects of rGO sheets.

Thus, it is crucial to properly select the interfacial interaction molecule to assist the dispersion of GE-based materials. The surfactant has stabilized GO sheets more in the nanocomposite and thus can increase the effective platform for ion kinetics movements between the electrodes and the electrolyte. Moreover, the tail group at the hydrophobic part of the surfactant was also responsible for the specific capacitance increment. The increasing number of tail groups might believe to help and assist carbon group more effective in the NRL polymer. Thus, a more convenient, green, and simple approach to fabricate nanocomposite with similar or beyond the electrical conductivity reported and improved capacitive behavior needs to be seriously investigated.

Therefore, in this chapter, the aim of the work is to further discuss on the effects of different type of surfactants in GO production. The work was systematically performed and discussed accordingly throughout the chapter. The synthesize of GO were carried out using commercially available surfactant of single-tail (SDS, SDBS, PSS) and custom-made surfactants of double- (AOT4) and triple-tails (TC14) at 7 V (0.1 M) for 24 hours synthesis process via electrochemical exfoliation method [21, 22]. Meanwhile, the nanocomposite samples were fabricated using one-step approach of electrochemical exfoliation as reported previously [23, 24]. The performance of all samples was discussed in terms of its electrical and capacitive behavior.

2. Graphene oxide assisted single-, double-, and triple-tails of surfactants

In this part, the characterizations of GO production using various surfactants were demonstrated; including morphological surfaces (FESEM), quality and defects level (Raman), absorption properties (UV-Vis). This stage is very important for quality and quantity evaluation of synthesized GO before incorporated with NRL polymer latex. All samples were measured using field emission scanning electron microscopy (FESEM- Hitachi SU 8020), micro-Raman spectroscopy (Renishaw InVia Raman Microscope), UV-Vis spectroscopy (Agilent 8453 Spectrophotometer).

2.1 Morphological characterization

FESEM is the most important tool to figure out the morphological characteristics of GO produced. From the FESEM images, the GO samples synthesized using 0.1 M of various surfactants are presented in **Figure 1(a)–(e)** The commercially available single-tail surfactants of SDS, SDBS and PSS were the initial type of surfactant used for electrolyte preparation. Generally, these three single-tail surfactants gave a crumple layers of GO. Between those three single-tail surfactant (SDS, SDBS and PSS), the growth of well-structured GO was observed at sample prepared using SDS surfactant (**Figure 1(a)**). This was predicted due to the low-molecular surfactants that pack tightly on the GO surfaces for maximizing the surface charge

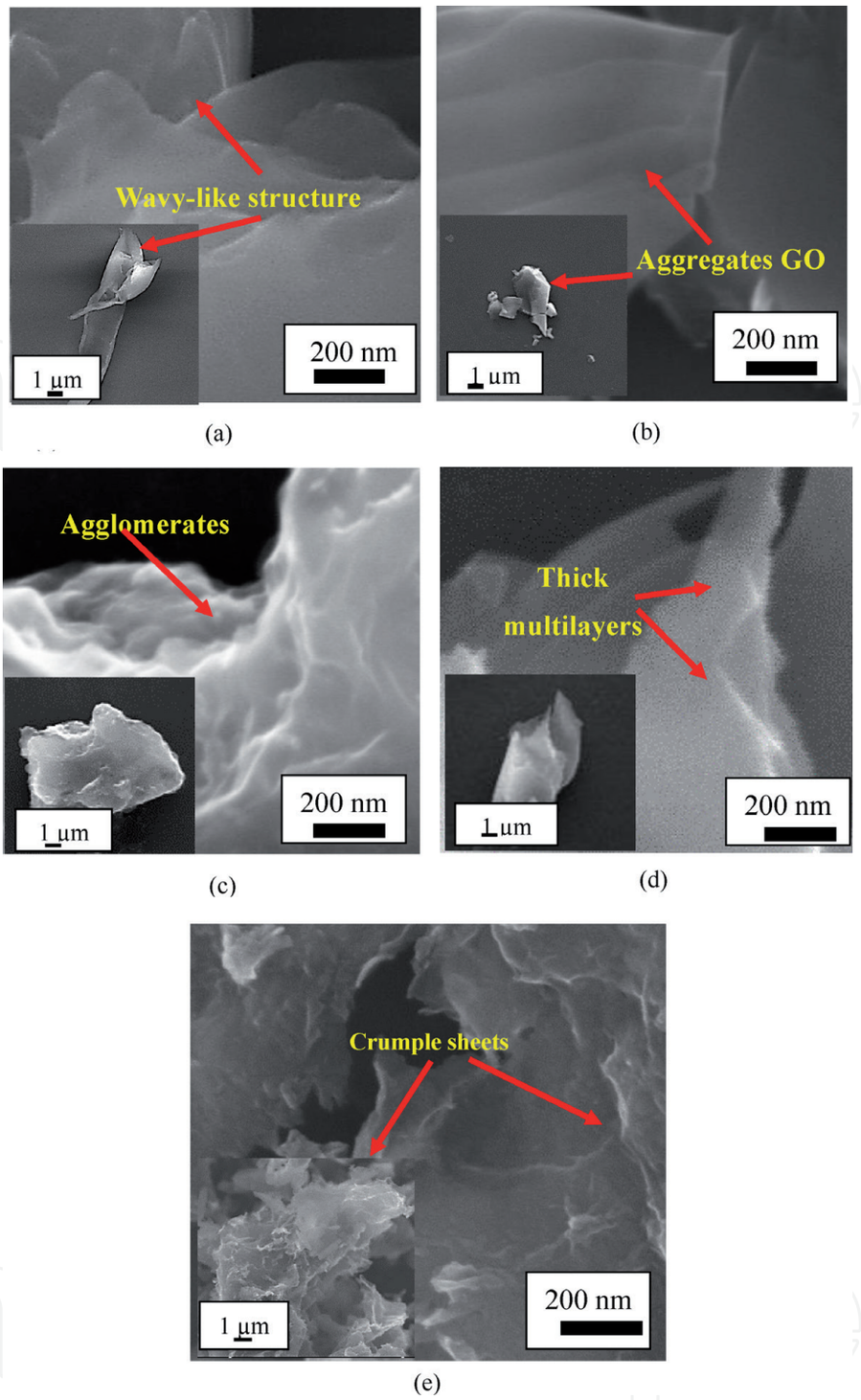

Figure 1.
FESEM images of 0.1 M-GO synthesized using different surfactants (a) SDS, (b) SDBS, (c) PSS, (d) AOT4, and (e) TC14 via electrochemical exfoliation method.

in the graphitic layers. This has led to the optimum exfoliated GO that can be achieved to be in the dispersions [25, 26].

Meanwhile, the SDBS-GO sample shows the fold up structure at the edges of GO sheets and the sample has the tendency to aggregate as compared to the SDS (shown in inset **Figure 1(b)**). This was probably because the benzene ring in the SDBS molecule causes a π-π interaction between molecules in addition to hydrophobic interaction between surfactant tails [27]. Therefore, at higher concentration of electrolyte, the number of the interactions between the surfactant and the GO sheets was increased which causes to the formation of aggregation GO sheets and stacked layers at the basal plane.

In addition, the PSS-GO sample (**Figure 1(c)**) also shows agglomerated structure of GO. This observation was due to the relatively weaker π-π interactions between the surfactant molecule and the GO surfaces thus did not effectively reduce the agglomeration of GO structures [28]. This shows that the benzene ring located in the head group of surfactant does not give significant effects to the GO produced due to the fact that the hydrophobic tails group was mainly responsible for the intercalation and interaction between the GO sheets and the tail group of the surfactant. This result was consistent with the fact that at higher electrolyte concentration which represents the high amount of surfactant, largely led to the agglomerations of GO sheets. Therefore, the use of single-tail surfactant (SDS, SDBS and PSS) at higher concentration only shows slightly improve in the GO dispersions with slightly higher GO volume produced. Due to the important role of the hydrophobic tails group surfactant in the exfoliation process of GO, the custom-made surfactant of double- and triple-tails of AOT4 and TC14, respectively was further investigated.

In comparison to the double- and triple-tails surfactant of AOT4 and TC14 as shown in **Figure 1(d** and **e)**, the TC14-GO sample produces at 0.1 M shows more crumpled structure as compared to the double-tails surfactant of AOT4-GO sample (**Figure 1(d)**). This might believe due to the triple-tails surfactant offers triple interaction and stabilization on the GO surfaces which led to the maximum exfoliated GO in the sample produced as compared to the single- (SDS, SDBS and PSS) and double-tails (AOT4) surfactant. At approximate volume of 0.1 M, the triple-tails of TC14 inserted helps to triple order separate the graphitic layers and prevent GO layers from reforming the π-π stacking interaction between the GO sheets. The lower surface tension of triple-tails TC14 (γ_{cmc} = 27.0 mN m^{-1}) attempting to minimize the hydrophobic interactions between GO layers which subsequently find the way to the gaps opening up at the edges more than the higher surface tension of single-tail SDS (γ_{cmc} = 34.7 mN m^{-1}). Due to the different surface tension of different surfactants, the single-tail surfactants were seen not sufficient to dislodge the graphite layers to individual sheets and bring the GO sheets into the water-based medium. Meanwhile, for double-tails surfactant, AOT4-GO sample shows a smooth GO surface exfoliated to the multilayers as pointed by arrows. However, the thick layers observed have convinced that the double-tails surfactant still beneath the sufficient level to successfully exfoliate the GO sheets to thin and transparent layers. Therefore, the length and greater branches of alkyl chains of surfactant play a role in the GO dispersions [28–30].

Micro-Raman spectroscopy has a sensitivity, and it is the most general technique to characterize the carbonaceous materials. This technique was important in order to observe the vibrational and rotational of the carbon materials. As previously discussed, it was well-known that higher crystallinity of the GO produced was shown by the higher intensity ratio of D- to G-peaks due to successful oxidation process [31]. On the other hand, the increased of the I_D/I_G ratio can also be measured as the increase of the defect levels of the sample. This can be reflected to the PSS-GO sample whereas the lowest I_D/I_G ratio of 0.64 and sharp 2D-peak at 2712.3 cm^{-1} has indicated the GO sample can also produce a better crystallinity at higher concentration. The obviously intense shape of the 2D-peak in PSS-GO dispersions shows that the dispersions were also consisted by several single GE layers [32, 33]. However, the PSS-GO sample has shown the additional band (G+ band) which detected at ~1620 cm^{-1} represented the edge defects. This additional peak was corresponded to the edges of GO sheets fold up due to the π-π interaction between the aromatic rings of the surfactant and the GO sheets. This resulted from the low energy of the surfactant used to exfoliate GO at the edges part by using higher electrolyte concentration (0.1 M). The repetition on micro-Raman measurement of PSS-GO sample

shows that the calculated I_D/I_G ratio value were not consistent across the samples suggesting low structural uniformity. The observation has been supported by the FESEM where the sample has formed an agglomerates GO sheets and less uniformity. Due to this, the single-tail surfactant of PSS was not included in the next GO growth parameter.

Meanwhile, for SDBS-GO sample, a faint G+ band was observed at around ~1639 cm^{-1} in the SDBS-GO sample. This shows that the single-tail surfactants of SDBS and PSS were not enough to exfoliate the GO sheets into the single and thin layers of GO. Meanwhile, by increasing the number at the tail group of surfactant from double- (AOT4) to triple-tails (TC14), the decrease pattern of I_D/I_G ratio was observed which were calculated to be 0.88 and 0.82, respectively. The moderate quantity and quality of the TC14-GO sample indicated that the triple-tails surfactant shows a great improvement in the exfoliating and stabilizing GO sheets. This might be explained by the triple interactions of surfactant to assist the production of GO sheets via electrochemical exfoliation method.

In addition, less intense 2D-peak appeared in the TC14-GO sample at around 2715.8 cm^{-1} shows that the GO produced also consists of few layer GO sheets. However, the biggest 2D-peak width (96.3 cm^{-1}) indicated that the GO sheets were highly stabilized by the triple-tails TC14 surfactant thus increased the interlayer spacing of GO layers. In comparison, upon the introduction of single- and double-tails surfactant of SDS and AOT4 assisted in the GO production, a broad and weak 2D-peak (~2712.8–2718.0 cm^{-1}) were detected which indicates that the GO produced has a slightly higher of structural disorder of GO [35]. The details have been shown in **Figure 2** and **Table 1**. The results were consistent with the FESEM analysis as discussed above where the number of tail group and the electrolyte concentration of surfactant plays an important role in the high yield and better GO sample production and stabilization.

UV-Vis absorption measurement was conducted on the synthesized GO and is shown in **Figure 3**. The absorption peaks at around ~223–232 nm in the UV-Vis spectrum was detected in the synthesized GO using single- (SDS, SDBS and PSS),

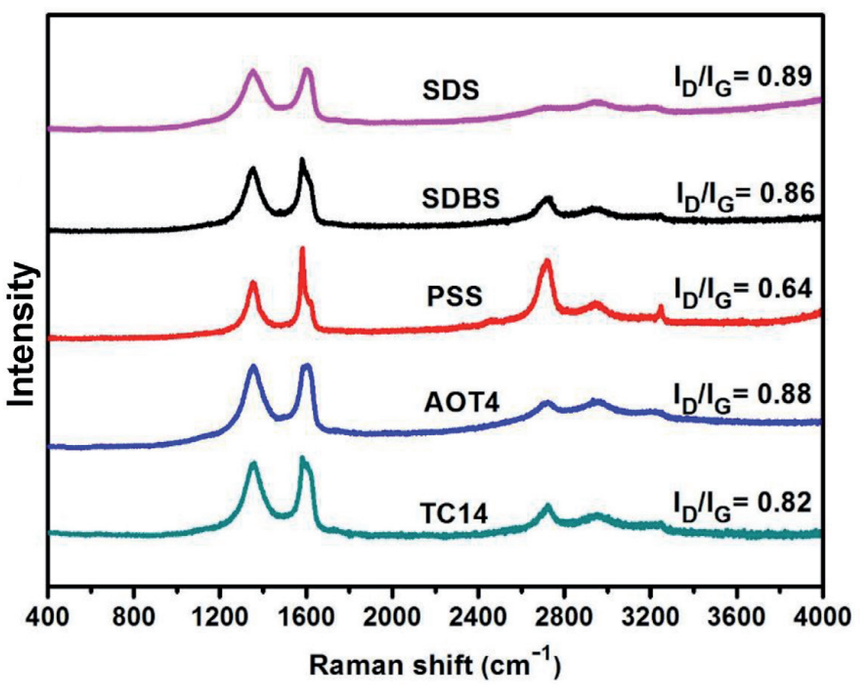

Figure 2.
Micro-Raman analyses of GO production using 0.1 M at various types of surfactant (SDS, SDBS, PSS, AOT4, and TC14) via electrochemical exfoliation method [34].

Samples: Different surfactants	G-peak (cm^{-1})	G-peak width (cm^{-1})	D-peak (cm^{-1})	D-peak width (cm^{-1})	I_D/I_G ratio	2D-peak	2D-peak width (cm^{-1})
0.1 M SDS-GO	1598.2	58.5	1357.0	97.7	0.89	2712.8	59.3
0.1 M SDBS-GO	1590.7	61.4	1353.3	91.2	0.86	2716.6	57.7
0.1 M PSS-GO	1582.3	26.9	1353.2	48.4	0.64	2712.3	73.2
0.1 M AOT4-GO	1597.6	59.4	1357.6	89.9	0.88	2718.0	69.7
0.1 M TC14-GO	1595.5	65.8	1358.3	120.2	0.82	2715.8	96.3

Table 1.
Micro-Raman analyses for GO produced using 0.1 M at various types of surfactant (SDS, SDBS, PSS, AOT4, and TC14) via electrochemical exfoliation method.

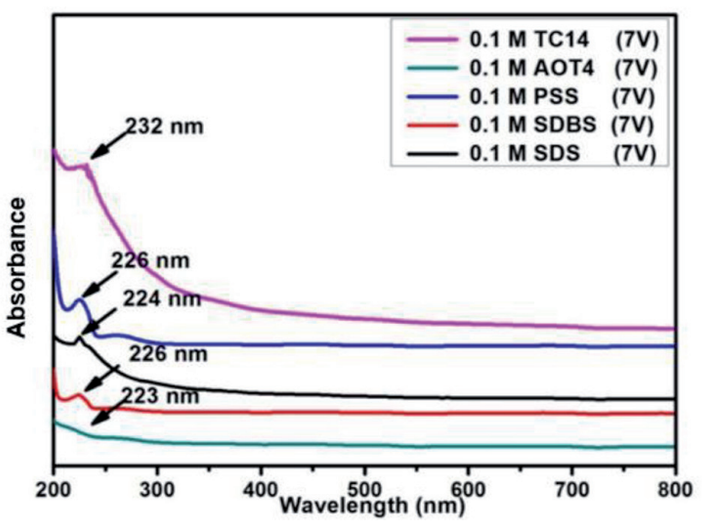

Figure 3.
UV-Vis spectra of GO produced using 0.1 M for different type of surfactants (SDS, SDBS, PSS, AOT4, and TC14) via electrochemical exfoliation method.

double- (AOT4) and triple-tails (TC14) surfactant. In comparison to the lower electrolyte concentration of 0.01 M, overall samples show the shifted peak to a high wavelength except for the sample prepared using SDS and AOT4 surfactant. It can be noted that at higher electrolyte concentration, the amount of GO produced has increased thus increasing the formation of various oxygen functional groups as confirmed by the slightly shifted peak to higher wavelength in UV-Vis.

Meanwhile, the prepared TC14-GO sample shows the obvious shifted peak of GO from 220 nm to highest wavelength of 232 nm as compared with other GO samples which attributes a high level of stability achieved by the GO dispersions [36]. On the other hand, the shifted peak at higher wavelength also as indicator of good dispersion of GO sheet where the largest amount of exfoliated GO was suspended in the water [35]. This characteristic shows that the triple-tails surfactant TC14 maintained the high ability to stabilize the GO sheets at both low (0.01 M) and high (0.1 M) electrolyte concentration. By increasing the electrolyte concentration from 0.01 to 0.1 M, the synthesized TC14-GO sample possesses the highest consistency in term of stabilization of GO sheets. In addition, it was believed that the nanoplatelets GE were also produced instead of sheets structures in the sample [36].

This information might be beneficial to the increase the interactions thus leading to the enhancement in electrical conductivity and capacitance performance.

In conclusion, GO synthesized using 0.1 M of triple-chain TC14 surfactant was successfully produced a highly crumpled structure with moderate crystallinity (I_D/I_G = 0.82) as compared to the single-chain SDS surfactant where a slightly higher crystallinity (I_D/I_G = 0.89). The triple-chain TC14 surfactant probably has well-stabilized the exfoliated GO sheets as compared to the single-chain SDS during the electrochemical exfoliation method. The triple-tails of TC14 might give the triple interactions to the GO production thus increasing the stabilization of GO sheets. These results have been confirmed by the UV-Vis analysis by the shifted peak from 220 to 232 nm. Therefore, GO-assisted triple-tails TC14 surfactant was considered as the suitable surfactant for higher quality and reasonably good graphitized GO as compared to single- (SDS) and double-tails (AOT4) surfactant.

3. Graphene oxide/natural rubber latex polymer nanocomposite synthesized via one-step method using different type surfactants

The one-step approach was implemented due to a simpler and rapid production of GE-based electrodes. Through the one-step, upon the production of GO solution, latex milk was simultaneously mixed in the exfoliation system for overnight. The obtained sample was dried for 24 hours in a petri dish to form a thin film. This work has been performed as previously discussed [37, 38]. The electrical conductivity and capacitive behavior was done using four-point probe (Keitley 2636A), and cyclic voltammetry (CV-Gamry potentiostat series-G750 equipped galvanostat) measurements, respectively. Moreover, the morphological characterization using FESEM was also discussed in this section in order to support the stability information of the electrodes produced.

3.1 Electrical enhancement

Figure 4 depicts the electrical conductivities of the TC14-GO/NRL and SDS-GO/NRL polymer nanocomposite. The *I-V* curves presented in **Figure 4** revealed that increasing the number of single-tail SDS to triple-tail TC14 surfactant led to significant enhancement of electrical conductivity. This finding was consistent with

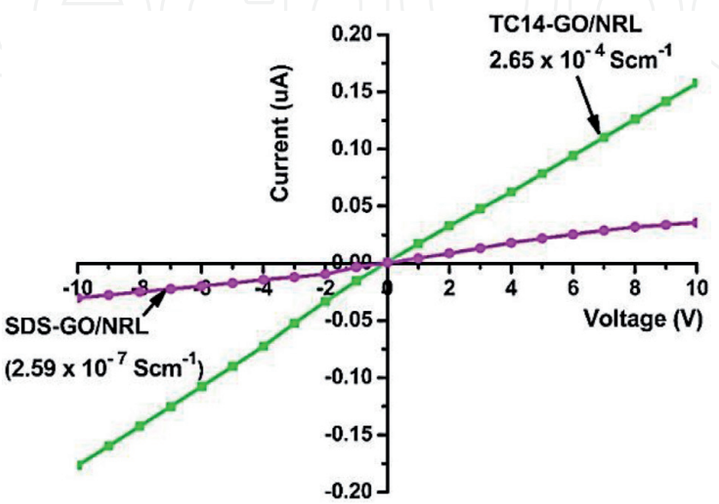

Figure 4.
I-V *curves of the 0.1 M GO/NRL polymer nanocomposite stabilized using SDS and TC14 surfactant synthesized via one-step method of electrochemical exfoliation.*

that of Mohamed et al. in dispersing CNT in the NRL matrix by the latex technology approach [29]. The presence of TC14 surfactant resulted in the high electrical conductivity range (2.65×10^{-4} S cm^{-1}) compared with the single-chain SDS surfactant (2.59×10^{-7} S cm^{-1}). This result showed that the triple-chain TC14 surfactant assisted in the formation of conductive pathways between the GO and NRL matrix [39]. The conductive network was formed by allowing the hydrophobic part of the surfactant to adsorb and interact with the GO structures, thereby decreasing the surface charge of the carbon material [40]. Therefore, the electrical conductivity improvement of the GO/NRL polymer nanocomposite was strongly affected by the tail group of the surfactant, which was believed to improve the dispersions between GO and NRL polymer. This result suggests that the nature of surfactant plays an important role to obtain GO/NRL polymer nanocomposite with significantly higher electrical conductivities. This finding was also supported by the capacitance behavior where the TC14-GO/NRL polymer nanocomposite samples showed high current response and large leaf shape.

3.2 Capacitance performance

Figure 5(a) and **(b)** shows the *C-V* curves of TC14-GO/NRL polymer nanocomposite prepared at a scan rate of 100 m Vs^{-1}. A high capacitance value of 25 F g^{-1} was measured for the TC14-GO/NRL polymer nanocomposite sample as compared to the SDS-GO/NRL polymer nanocomposite sample (5 F g^{-1}). The triple-tails surfactant, TC14 shows the higher influence on the capacitance behavior of GO/NRL polymer nanocomposite as compared to single-tail surfactant, SDS. The resulted capacitance obtained was due from good ion propagation between the TC14-GO/NRL polymer nanocomposite electrodes and the electrolyte. This might be explained as the single-tail SDS surfactant has low interaction with ratio 1:1 between the GO sheets and the NRL polymer matrix as compared to the triple-tails TC14 surfactant where triple-tails surfactant has triple interactions to GO sheets with ratio 3:1. In addition, the low capacitive performance obtained shows that at higher concentration of electrolyte (0.1 M), more agglomerations formed were led to the higher resistivity of the ion transfer between the electrolyte and electrodes. Therefore, the triple-tails TC14 surfactant has built triple pathways for ions diffusion between the electrodes and the electrolyte. The remained surfactant in the nanocomposite has efficiently prevented aggregation and restacking of GO upon cyclic measurement. Furthermore, the single-tail SDS surfactant also has low ion mobility in aqueous solution which limited the charge diffusion between the electrodes and the electrolyte [41]. The type of surfactant used has great influenced on the ions mobility of medium within the electrolyte.

However, the *C-V* curves of both GO/NRL polymer nanocomposite shows slightly distortion of the leaf-like shape, indicating that the surfactants introduced have positive effect on capacitance behavior of the nanocomposite electrode. It also can be seen from **Figure 5** that with the addition of triple-tails surfactant, TC14, the *C-V* curve becomes broader which subsequently improved the capacitance behavior. These results indicated that the TC14-GO/NRL polymer nanocomposite produced have great potential to be implemented as green and low-cost supercapacitor electrodes.

In the CD curves, the longer discharge time than the charging time at low current density implies an asymmetric behavior in charging and discharging section, due to the redistribution of charges after charging the electrode [42, 43]. From the results (**Figure 6**), the charging and discharging time pattern showed a symmetric behavior, which concluded that both electrodes have potential in restoring the charges. However, in comparison, the sample consisted triple-tails,

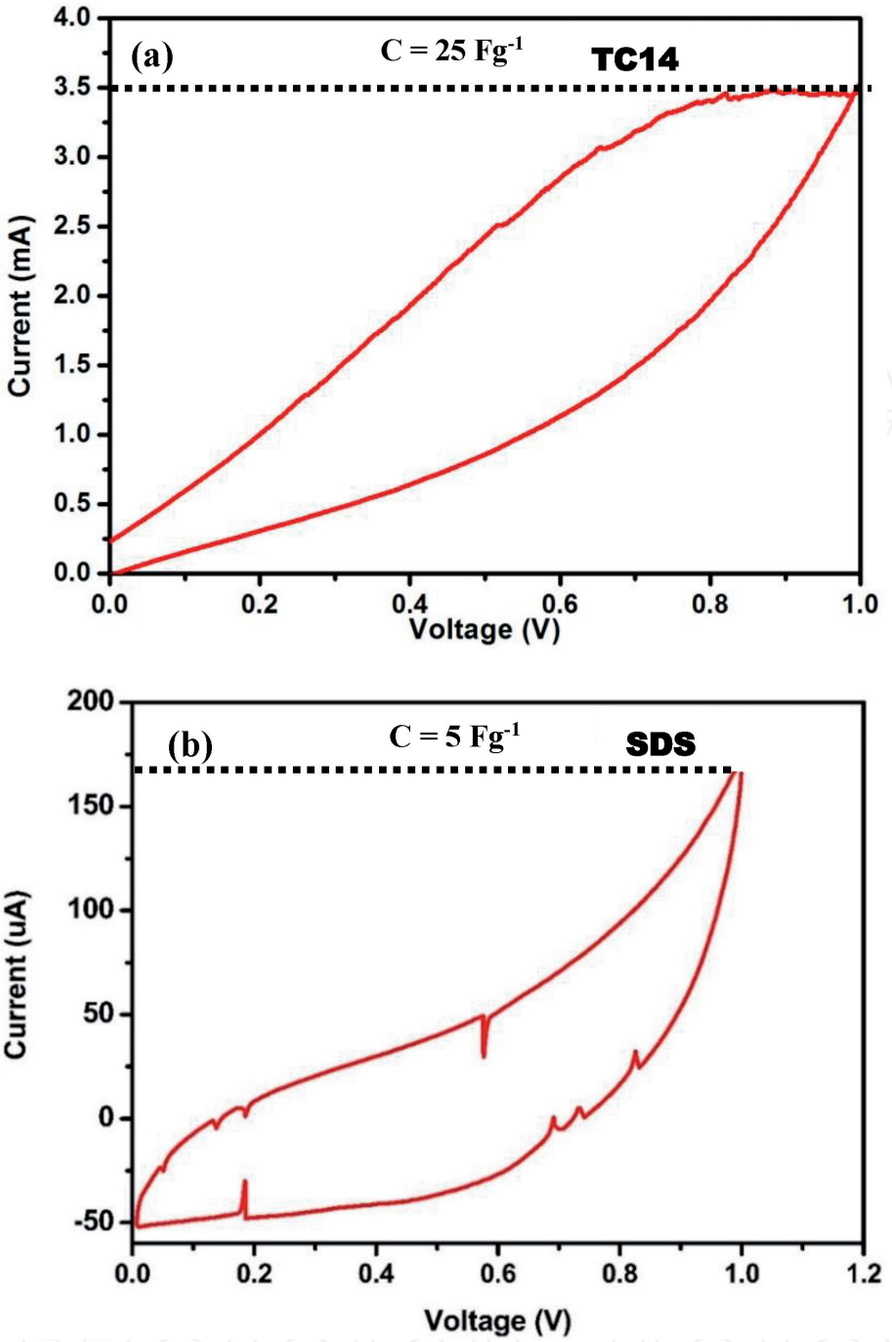

Figure 5.
C-V *curves of the (a) TC14-GO/NRL and (b) SDS-GO/NRL polymer nanocomposite synthesized via one-step method of electrochemical exfoliation.*

TC14 (**Figure 6(a)**) showed a distortion pattern between charging and discharging time which probably due to the high surface redox reaction of oxygen-containing functional groups [44, 45]. This was supported by the specific capacitance obtained by both nanocomposites. Meanwhile, the low specific capacitance observed by the sample of 0.1 M SDS-GO/NRL was expected due to the jumbled distribution of GO samples on the NRL matrix surface which was supported by FESEM image. This has led to the increment of resistance of both charge transport and electrolyte ions diffusion [46]. The crack formation between the GO sheets and NRL polymer after cycling process also convinced that the nanocomposite has low interaction. However, in general, the discontinuous conductive network between the GO sheets assisted surfactant in the NRL matrix also bring to the low of specific capacitance and charge-discharge pattern.

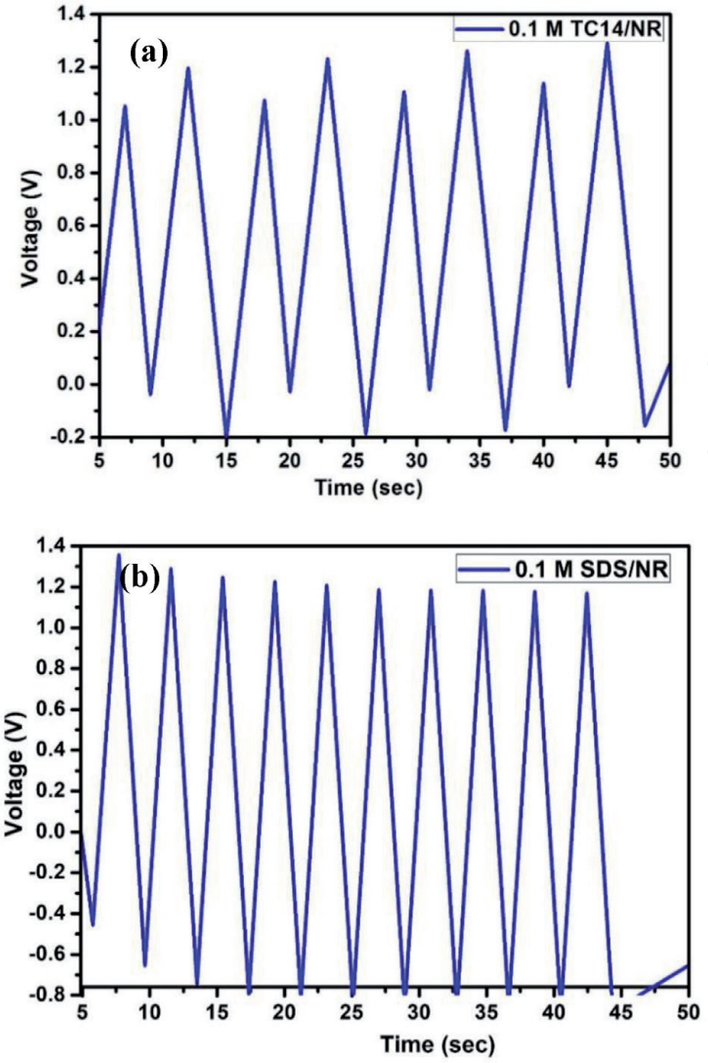

Figure 6.
C-D *curves of the (a) TC14-GO/NRL and (b) SDS-GO/NRL polymer nanocomposite synthesized via one-step method of electrochemical exfoliation.*

3.3 Morphology characterization

Figure 7 shows the cross-sectional FESEM images of the SDS-GO/NRL and TC14-GO/NRL polymer nanocomposite samples were studied to investigate the dispersion of the GO sheets assisted surfactant into the NRL polymer matrix. The figure clearly demonstrations that both the nanocomposite samples show dispersion of the few layers of exfoliated GO sheets throughout the NRL matrix. Dispersion GO assisted triple-tails surfactant, TC14 plays a significant role to fabricate high performance GO/NRL polymer nanocomposite. As reported in previous work [47], a good dispersion in the polymer matrix can be achieved by including surfactant in the composite materials. This was due to the improvement in the hydrophobic interaction between the surfactant and GO sheets layer, thus lowering the van der Waals between the graphene sheets. After sometimes of cycling testing, a crack surface in SDS-GO/NRL polymer nanocomposites sample observed in between the agglomerated GO sheets and polymer matrix (**Figure 7a**). This might contribute to the decreasing patent of charging-discharging measurement (C-D curve in **Figure 6**). In comparison, the higher dispersion achieved by the TC14-GO/NRL nanocomposites and higher stability in C-D curve showed that a great influence of high branches surfactant in increasing the long-time stability of the nanocomposite

produced. A bulk GO sheets observed confirmed a higher interaction of triple-tails TC14 to the GO surfaces, thus consequence to the bulk agglomerated GO.

Figure 8 gives the illustration of the GO sheets produced using single-tail surfactant of SDS at both low (0.01 M) and high (0.1 M) electrolyte concentration.

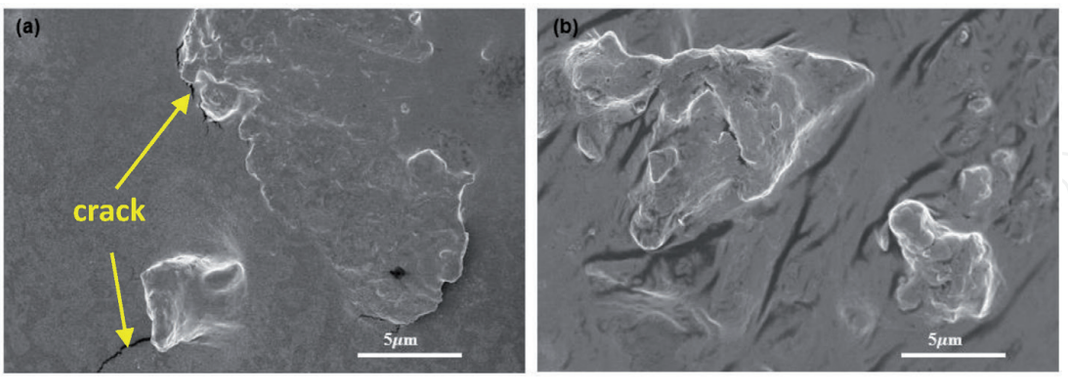

Figure 7.
FESEM images of the (a) SDS-GO/NRL and (b) TC14-GO/NRL polymer nanocomposite synthesized via one-step method of electrochemical exfoliation. Noted that the GO sheets are shown by the pull out bulk particle from the smooth NRL matrix.

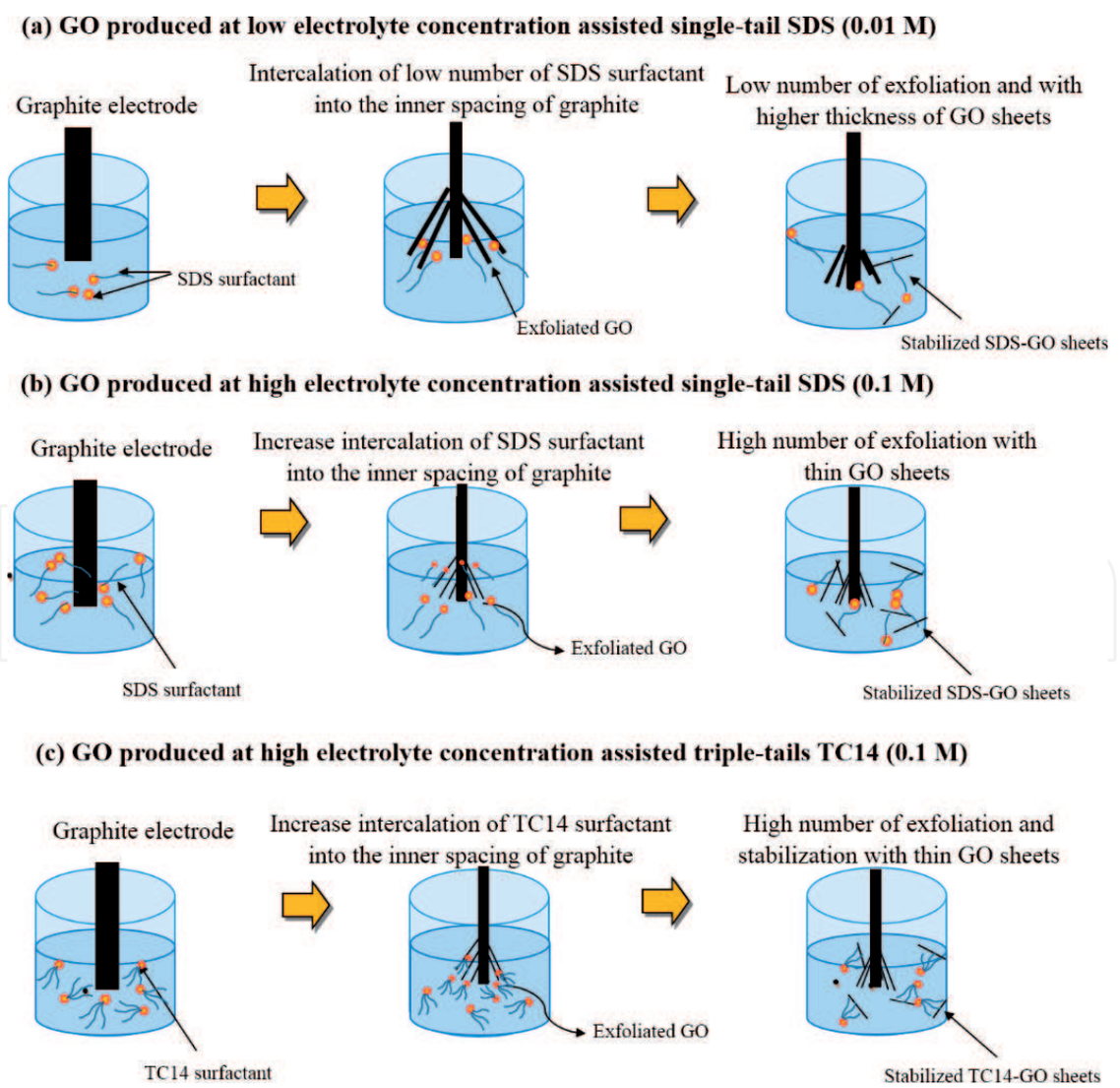

Figure 8.
Illustration of (a) 0.01 M SDS-GO, (b) 0.1 M SDS-GO, and (c) 0.1 M TC14-GO samples produced via electrochemical exfoliation method.

The schematic diagram in **Figure 8(a)** shows that the SDS surfactant has exfoliated the graphite into several layers of GO. At low electrolyte concentration of 0.01 M SDS, the low number of SDS surfactant yielded low amount of GO produced. The low number of surfactant has caused to the insufficient energy to successfully exfoliate the GO layers into thin sheets thus produced an agglomerate and thick GO sheets. As compared to high electrolyte concentration of 0.1 M (**Figure 8 (b)**), the higher number of SDS surfactant has increased the amount of exfoliated GO sheets in the dispersion. This was due to the sufficient energy of SDS at above critical micelle concentration (CMC) level to exfoliate graphite into multilayers of GO and the SDS has further stabilized the layers as shown in **Figure 8(b)** Due to the strong van der Waals interaction between the GO layers, the highly exfoliated layers of GO has tends to stack on top of the GO layers thus producing thicker GO sheets with numerous wrinkles. This illustration was consistent with the FESEM images where the produced GO at high concentration (0.1 M) has slightly bulk layers indicates high number of exfoliated GO. Meanwhile, **Figure 8(c)** compares the greater branches of triple-tails surfactant, TC14 assisted in the GO production using electrolyte concentration of 0.1 M with the commercially available single-tail, SDS surfactant (0.1 M). At above of CMC level of TC14 surfactant (0.1 M), the TC14 surfactant provides triple order interaction and higher stabilization between the triple-tails surfactant with the GO sheets thus produced higher volume and great quality of GO sheets compared to SDS-GO. The use of triple-tails surfactant of TC14 at and above the CMC level may facilitates the similar triple interaction to the GO sheets in both aqueous and non-aqueous electrolytes where the TC14 has shown important role in determining the number of thin GO sheets with higher stabilization of the GO layers produced.

4. Conclusion

Various analytical techniques done revealed that the GO produced were strongly affected by the surfactants used (TC14, AOT4, SDBS, PSS and SDS). TC14 surfactant was considered the most suitable surfactant for higher quantity and reasonably good graphitized GO (I_D/I_G = 0.82–0.83). Due to the high quantity and quality of GO produced using triple-tails TC14 surfactant, a close comparison was done with the single-tail SDS surfactant in order to investigate the performance of GO-assisted surfactant in the NRL polymer nanocomposite. The one-step method with 24 hours of synthesis time was carried out at 7 and 10 V using 0.1 and 0.01 M, respectively, throughout this work. The initial analysis was done by measuring the electrical properties of GO filled NRL nanocomposites then followed by capacitance and structural properties. This was due to the samples were bench making by its electrical conductivity then only capacitance and structural properties.

Acknowledgements

The author wants to acknowledge Short Term Grant, Universiti Sains Malaysia (USM, Penang) (304/PFIZIK/6315241) that has made this research possible. Special thanks to Nano-Optoelectronics Research and Technology Laboratory, School of Physics (USM) and Nanotechnology Research Centre, Universiti Pendidikan Sultan Idris (UPSI) for their facilities support. Author is thankful to Malaysian Rubber Board industry for latex supplied and many thanks to Associate Professor Dr. Azmi Mohamed for the custom-made surfactants supplied in this study.

Conflict of interest

The authors declare no conflict of interest.

Author details

Nurhafizah Md Disa
School of Physics, Universiti Sains Malaysia, USM Penang, Malaysia

*Address all correspondence to: mdnurhafizah@usm.my

References

[1] Novoselov KS, Geim AK, Morozov SV, Jiang D, Katsnelson MI, Grigorieva I, et al. Two-dimensional gas of massless dirac fermions in graphene. Nature. 2005;**438**:197-200. DOI: 10.1038/nature04233

[2] Morozov SV, Novoselov KS, Katsnelson MI, Schedin F, Elias DC, Jaszczak JA, et al. Giant intrinsic carrier mobilities in graphene and its bilayer. Physical Review Letters. 2008;**100**(1):016602. DOI: 10.1103/PhysRevLett.100.016602

[3] Lee C, Wei XD, Kysar JW, Hone J. Measurement of the elastic properties of intrinsic strength of monolayer graphene. Science. 2008;**321**:385-388. DOI: 10.1126/science.1157996

[4] Zhang Y, Small JP, Amori MES, Kim P. Electric field modulation of galvanomagnetic properties of mesoscopic graphite. Physical Review Letters. 2005;**94**(17):176803. DOI: 10.1103/PhysRevLett.94.176803

[5] Kim KS, Zhao Y, Jang H, Lee SY, Kim JM, Kim KS, et al. Large-scale pattern growth of graphene films for stretchable transparent electrodes. Nature. 2009;**457**:706-716. DOI: 10.1038/nature07719

[6] Yang S-Y, Chang K-H, Lee Y-F, Ma C-CM HC-C. Constructing a hierarchical graphene-carbon nanotube architecture for enhancing exposure of graphene and electrochemical activity of Pt nanoclusters. Electrochemistry Communications. 2010;**12**(9):1206-1209. DOI: 10.1016/j.elecom.2010.06.020

[7] Ghislandi M, Tkalya E, Schilinger S, Koning CE, De With G. High performance graphene-and MWCNTs-based PS/PPO composites obtained via organic solvent dispersion. Composites Science and Technology. 2013;**80**:16-22. DOI: 10.1016/j.compscitech.2013.03.006

[8] Matos CF, Galembeck F, Zarbin F, Aldo JG. Multifunctional and environmentally friendly nanocomposites between natural rubber and graphene or graphene oxide. Carbon. 2014;**78**:469-479. DOI: 10.1016/j.carbon.2014.07.028

[9] Zhan Y, Lavorgna M, Buonocore G, Xia H. Enhancing electrical conductivity of rubber composites by constructing interconnected network of self-assembled graphene with latex mixing. Journal of Materials Chemistry. 2012;**22**(21):10464-10468. DOI: 10.1039/C2JM31293J

[10] Stankovich S, Dikin DA, Dommett GHB, Rohlhaas KM, Zimney EJ, Stach EA, et al. Graphene-based composite material. Nature. 2006;**442**:282-286. DOI: 10.1038/nature04969

[11] Nurhafizah MD. Magnetic properties of graphene oxide via a simple mixing with waste engine oil-based carbon nanotubes. SN Applied Sciences. 2020;**2**:534. DOI:10.1007/s42452-020-2361-8

[12] Shah RK, Hunter DL, Paul DR. Nanocomposites from poly (ethylene-co-methacrylic acid) ionomers: Effect of surfactant structure on morphology and properties. Polymer. 2005;**46**(8):2646-2662. DOI: 10.1016/j.polymer.2005.01.062

[13] Guo B, Tang Z, Zhang L. Transport performance in novel elastomer nanocomposites: Mechanism, design and control. Progress in Polymer Science. 2016;**61**:29-66. DOI: 10.1016/j.progpolymsci.2016.06.001

[14] Aguilar-Bolados H, Brasero J, Lopez-Manchado MA, Yasdani-

Pedram M. High performance natural rubber/thermally reduced graphite oxide nanocomposites by latex technology. Composites Part B: Engineering. 2014;**67**:449-454. DOI: 10.1016/j.compositesb.2014.08.010

[15] Zuberi M, Sherman DM, Cho Y. Carbon nanotube microspheres produced by surfactant-mediated aggregation. The Journal of Physical Chemistry C. 2011;**115**(10):3881-3887. DOI: 10.1021/jp110019e

[16] Mohamed A, Anas AK, Suriani AB, Ardyani T, Zin WMW, Ibrahim S, et al. Enhanced dispersion of multiwall carbon nanotubes in natural rubber latex nanocomposites by surfactants bearing phenyl groups. Journal of Colloid and Interface Science. 2015;**455**:179-187. DOI: 10.1016/j.jcis.2015.05.054

[17] Mohamed A, Ardyani T, Suriani AB, Brown P, Hollamby M, Sagisaka M, et al. Graphene-philic surfactants for nanocomposites in latex technology. Advances in Colloid and Interface Science. 2016;**230**:54-69. DOI: 10.1016/j.cis.2016.01.003

[18] Zhou S, Wei D, Shi H, Feng X, Xue K, Zhang F, et al. Sodium dodecyl benzene sulfonate functionalized graphene for confined electrochemical growth of metal/oxide nanocomposites for sensing application. Talanta. 2013;**107**:349-355. DOI: 10.1016/j.talanta.2013.01.041

[19] Yuan K, Xu Y, Uihlein J, Brunklaus G, Shi L, Heiderhoff R, et al. Straightforward generation of pillared, microporous graphene frameworks for use in supercapacitors. Advanced Materials. 2015;**27**(42):6714-6721. DOI: 10.1002/adma.201503390

[20] Jothi PR, Salunkhe RR, Pramanik M, Kannan S, Yamauchi Y. Surfactant-assisted synthesis of nanoporous nickel sulfide flakes and their hybridization with reduced graphene oxides for supercapacitor applications. RSC Advances. 2016;**6**(25):21246-21253. DOI: 10.1039/C5RA26946F

[21] Nurhafizah MD, Khor SY, Tan KL, Soga T. The synthesized reduced graphene oxide enhanced the capacitive behavior of activated carbon/pva as potential electrode materials. Journal of Nanostructures. 2019:**2**(10)1. DOI: 10.22052/jns.2019.196289.1919

[22] Nurhafizah MD, Suriani AB, Alfarisa S, Mohamed A, Isa IM, Kamari A, et al. The synthesis of graphene oxide via electrochemical exfoliation method. Advanced Materials Research. 2015;**1109**:55-59. DOI: 10.4028/www.scientific.net/amr.1109.55

[23] Nurhafizah MD, Suriani AB, Mohamed A, Soga T. Effect of voltage applied for graphene oxide/latex nanocomposite produced via electrochemical exfoliation and its application as conductive electrodes. Diamond and Related Materials. 2020;**101**:107624. DOI: 10.1016/j.diamond.2019.107624

[24] Nurhafizah MD, Aziz AA, Suriani AB, Mohamed A, Soga T. Low-temperature exfoliated graphene oxide incorporated with different types of natural rubber latex: Electrical and morphological properties and its capacitance performance. Ceramics International. 2020;**46**(5):5610-5622. DOI: 10.1016/j.ceramint.2019.11.005

[25] Smith RJ, Lotya M, Coleman JN. The importance of repulsive potential barriers for the dispersion of graphene using surfactants. New Journal of Physics. 2010;**12**:125008. DOI: 10.1088/1367-2630/12/125008

[26] Sun Z, Nicolosi V, Rickard D, Bergin SD, Aherne D, Coleman JN. Quantitative evaluation of surfactant-stabilized single-walled carbon nanotubes: Dispersion quality and its

correlation with zeta potential. Journal Physics Chemistry C. 2008;**112**:10629-10638. DOI: 10.1021/jp8021634

[27] Alemdar A, Gungor N, Erim FB. Effect of sodium dodecyl sulphate and sodium dodecyl benzene sulfonate on the flow behavior of purified bentonite dispersion. Journal of Materials Science Letters. 2003;**22**:89-90. DOI: 10.1023/A:1021836115359

[28] Cai X, Zhang Q, Wang S, Pen J, Zhang Y, Ma H, et al. Surfactant-assisted synthesis of reduced graphene oxide/polyaniline composites by gamma irradiation for supercapacitors. Journal of Materials Science. 2014;**49**(16):5667-5675. DOI: 10.1007/s10853-014-8286-0

[29] Mohamed A, Anas AK, Suriani AB, Azira AA, Sagisaka M, Brown P, et al. Preparation of multiwall carbon nanotubes (MWCNTs) stabilised by highly branched hydrocarbon surfactants and dispersed in natural rubber latex nanocomposites. Colloid & Polymer Science. 2014;**292**(11):3013-3023. DOI: 10.1007/s00396-014-3354-1

[30] Mohamed A, Trickett K, Chin SY, Cummings S, Sagisaka M, Hudson L, et al. Universal surfactant for water, oils, and CO2. Langmuir. 2010;**26**(17):13861-13866. DOI: 10.1021/la102303q

[31] Qiao SJ, Xu XN, Qiu Y, Xiao HC, Zhu YF. Simultaneous reduction and functionalization of graphene oxide by 4-hydrazinobenzenesulfonic acid for polymer nanocomposites. Nanomaterials. 2016;**6**(2):29. DOI: 10.3390/nano6020029

[32] Ferrari AC, Meyer JC, Scardaci V, Casiraghi C, Lazzeri M, Mauri F, et al. Raman spectrum of graphene and graphene layers. Physical Review Letters. 2006;**97**:187401. DOI: 10.1103/PhysRevLett.97.187401

[33] Graf D, Molitor FO, Ensslin K, Satmpfer C, Jungen A, Hierold C, et al. Spatially resolved Raman spectroscopy of single-and few-layer graphene. Nano Letters. 2007;**7**(2):238-242. DOI: 10.1021/nl061702a

[34] Nurhafizah Binti Md Disa. Synthesis of graphene oxide using electrochemical exfoliation method for electrode materials application. thesis dissertation; 2017

[35] Paredes JI, Burghard M, Martanez-Alonso TJMD. Graphitization of carbon nanofibers: Visualizing the structural evolution on the nanometer and atomic scales by scanning tunneling microscopy. Applied Physics A. 2005;**80**(4):675-682. DOI: 10.1007/s00339-004-3109-9

[36] Kazi SN, Badarudin A, Zubir MNM, Ming HN, Misran M, Sadeghinezhad E, et al. Investigation on the use of graphene oxide as novel surfactant to stabilize weakly charged graphene nanoplatelets. Nanoscale Research Letters. 2015;**10**(1):1-15. DOI: 10.1186/s11671-015-0882-7

[37] Suriani AB, Nurhafizah MD, Mohamed A, Zainol I, Masrom AK. A facile one-step method for graphene oxide/natural rubber latex nanocomposite production for supercapacitor applications. Materials Letters. 2015;**161**:665-668. DOI: 10.1016/j.matlet.2015.09.050

[38] Suriani AB, Nurhafizah MD, Mohamed A, Masrom AK, Mamat MH, Malek MF, et al. Electrical enhancement of radiation-vulcanized natural rubber latex added with reduced graphene oxide additives for supercapacitor electrodes. Journal of Materials Science. 2017;**52**:6611-6622. DOI: 10.1007/s10853-017-0897-9

[39] Potts JR, Shankar O, Du L, Ruoff RS. Processing-morphology-property relationships and composite theory analysis of reduced graphene oxide/natural rubber nanocomposites.

Macromolecules. 2012;**45**(15):6045-6055. DOI: 10.1021/ma300706k

[40] Clark MD, Subramanian S, Krishnamoorti R. Understanding surfactant aided aqueous dispersion of multi-walled carbon nanotubes. Journal of Colloid and Interface Science. 2011;**354**(1):144-151. DOI: 10.1016/j.cis.2010.10.027

[41] Ghasemi S, Hosseinzadeh R, Jafari M. MnO_2 nanoparticles decorated on electrophoretically deposited graphene nanosheets for high performance supercapacitor. International Journal of Hydrogen Energy. 2015;**40**(2):1037-1046. DOI: 10.1016/j.ijhydene.2014.11.072

[42] Graydon JW, Panjehshashi M, Kirk DW. Charge redistribution and ionic mobility in the micropores of supercapacitors. Journal of Power Sources. 2014;**245**:822-829. DOI: 10.1016/j.jpowsour.2013.07.036

[43] Andreas HA. Self-discharge in electrochemical capacitors: A perspective article. Journal of The Electrochemical Society. 2015;**162**(5):A5047. DOI: 10.1149/2.0081505jes

[44] He Y, Zhang Y, Li X, Lv Z, Wang X, Liu Z, et al. Capacitive mechanism of oxygen functional groups on carbon surface in supercapacitors. Electrochimica Acta. 2018;**282**:618-625. DOI: 10.1016/j.electacta.2018.06.103

[45] Kshetri T, Tran DT, Nguyen DC, Kim NH, Lau K, Lee JH. Ternary graphene-carbonnanofibers-carbonnanotubesstructureforhybridsupercapacitor. Chemical Engineering Journal. 2020;**380**:122543. DOI: 10.1016/j.cej.2019.122543

[46] Li T, Wang X, Liu P, Yang B, Diao S, Gao Y. Synthesis of graphene/polyaniline copolymer for solid-state supercapacitor. Journal of Electroanalytical Chemistry. 2020;**860**:113908. DOI: 10.1016/j.jelechem.2020.113908

[47] Layek RK, Uddin ME, Kim NH, Tak Lau AK, Lee JH. Noncovalent functionalization of reduced graphene oxide with pluronic F127 and its nanocomposites with gum Arabic. Composites Part B: Engineering. 2017;**128**:155-163. DOI: 10.1016/j.compositesb.2017.07.010